Proceedings of the 5th International Conference on Integrity-Reliability-Failure, Porto/Portugal 24-28 July 2016
Editors J.F. Silva Gomes and S.A. Meguid
Publ. INEGI/FEUP (2016)

PAPER REF: 6207

PLASTIC DEFORMATION DEGREE BASED ON VICKERS HARDNESS TEST NEAR THE FRACTURED SURFACES FOR DETERMINING J_{IC}

Viorel Goanta(*)
Technical University „Gheorghe Asachi", Bd. D. Mangeron 67, Iaşi, Romania
(*)*Email:* vgoanta@tuiasi.ro

ABSTRACT

As known, the degree of plastic deformation may be correlated with the value of the microhardness, determined in the plastically-deformed zone. The present paper discusses the testing applied, which led to the fracture of some specimens and, consequently, to plastic deformations in the immediate vicinity of the fractured surfaces. The testing, performed on Compact Tension Specimens, was aimed at determining the fracture toughness J_{Ic}. The Vickers microhardness number, determined in the immediate vicinity of the surfaces obtained through fracture, represents a faithful index for the determination of the degree of plastic deformation suffered by the material. Under such conditions, testing was made upon the 1C45 (1.053) steel, with the characteristics established by the manufacturer, as well as upon the same steel, yet subjected to an annealing thermal treatment, and the variations of Vickers microhardness were recorded both along the fractured surfaces and from one specimen to another.

Keywords: Fracture toughness, microhardness, plastic deformation, crack surface, J-integral.

THE HARDNESS NUMBER AS A MEASURE OF THE DEGREE OF PLASTIC DEFORMATION

Hardness can be defined as the property of a material to respond to the intrusion of a harder object in its superficial layers. Hardness is a measure for a certain material strength against plastic deformations, which may be also related to the yield stress. Parameters such as plastic deformation toughness, rigidity, residual stresses occurring in the vicinity of the surface and fracture toughness of a material may be evaluated by hardness tests, (Hahn, 1965, Hernas, 2001). Both hardness and tensile strength are indicators of metal toughness to plastic deformation. Commonly, a correlation between hardness and tensile strength is provided in literature, permitting an approximate estimation of steel tensile strength from its hardness value, (Pavlina, 2008). The hardness-tensile strength correlation is generally good (differences being usually less than ± 10 %). Cahoon et al. (Cahoon, 1971) offered expressions relating hardness, tensile strength and yield strength in the form of:

$$\sigma_{uts} = \frac{H}{2.9}\left(\frac{n}{0.217}\right)^n \tag{1}$$

$$\sigma_{ys} = \frac{H}{3}\cdot 0.1^n \tag{2}$$

where σ_{uts} and σ_{ys} stand for ultimate tensile strength and yield strength, respectively, and n is the strain-hardening exponent.

These expressions show excellent agreement (<2%) when calculating the tensile properties of a ferritic steel. Rolfe and Barsom, (Rolfe, 1987), developed a correlation between CVN (Charpy V-Notch) and fracture toughness (K_{Ic}), given by:

$$\left(\frac{K_{Ic}}{\sigma_{ys}}\right)^2 = 5\left(\frac{CVN}{\sigma_{ys}} - 0.05\right) \tag{3}$$

where K_{Ic} is fracture toughness at slow loading rates $(ksi(in)^{1/2})$, σ_{ys} is the 0.2% offset yield strength (ksi) and CVN is the standard Charpy V-Notch impact test value.

One of the key parameters characterizing the properties of yield stress is the strain-hardening exponent, n, for materials following the Hollomon equations, $\sigma=K\cdot\varepsilon^n$, where σ is the true stress, ε stands for the true strain and K is the strength coefficient. Kim et al. (Kim, 2008) consider the possibility of establishing a relation between the strain-hardening exponent, n, and the indentation size effect (ISE), represented by the characteristic length, h*. Different values for the strain-hardening exponent were obtained based on uniaxial tensile tests, which were interrupted in some point, at 5%, 10% and 15% values for Ni, and at 2% and 5%, respectively, for SCM21. The observation made for these materials was that the true stress–true strain curve follows the Hollomon equation. For both materials, an increased value of hardness at pre-loading level was noticed. The degree of deformation will be higher or lower, depending on the value and type of the loading applied in the moment in which the crack was propagated up to the zone considered for analysis and determination of the material properties.

Liu Zishun, (Liu, 2009) presents various techniques for the characterization of materials by taking into consideration the data provided by the loading (unloading) – displacement curve obtained based on the nanoindentations. A dimensionless analysis was used in order to establish a correlation between the characteristics of the nanoindentation curves and the properties of the materials. The calibration of the dimensionless functions was performed based on the finite elements analysis. A basic review of the first results is covered by Tabor (Tabor, 1951). Tabor has shown that the mean contact pressure P_m (or hardness) can be related to the yield stress σ_y or ultimate tensile strength R_m of the material, by an expression based on the theory of indentation of rigid-perfectly plastic solid.

In the literature, the Vickers hardness number (HV) has been the most popular element in the investigation of the relationship between the hardness and the lifetime or tensile strength of the material because of two reasons: firstly, its superior resolution compared to spherical indenters, and secondly, the Vickers indenter is self-similar, through which the hardness is ideally independent of the indentation load and indentation depth. Therefore, in this study, Vickers indentation will be as well the main concern. The relationship between Vickers hardness number and yield stress, as related to metal forming, is investigated by Dannenmann and Wilhelm (Dannenmann, 1958). As an observation based on the above-cited researches, it can be said that the experimental studies lack the separation of various factors affecting the hardness and lifetime or tensile strength relationship. On the other hand, the analytical and numerical studies lack either quantitative accuracy and/or they do not cover metal-forming issues properly.

In the present study, Vickers microhardness was determined along the surfaces fractured as a result of the load applied. Such tests support the idea that the material suffered differentiated

plastic deformations in the area from the immediate vicinity of the fractured surfaces. In order to check this, the test of Vickers microhardness is performed in the considered area.

CORRELATION BETWEEN THE HARDNESS AND THE DEGREE OF PLASTIC DEFORMATION USING THE TENSILE TESTING

One tries to establish if there is any possibility of quantifying the degree of plastic strain in relation to the value of the Vickers hardness of the specimen under stress, beyond the yield limit. A certain number of samples, with the same shape and geometry, were first tested at tensile, according to the standard specifications. Flat proportional specimens were used, with 6 mm in thickness and a gage length of 50 mm (Figure 1).

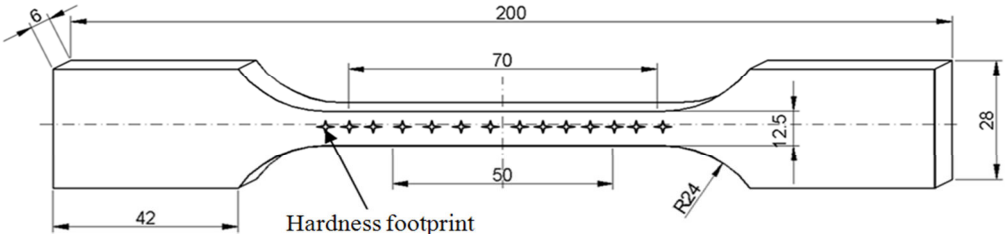

Fig. 1 - Typical shape of tensile test specimen

Figure 1 also presents the traces of the indentations which will be performed on samples for which the bottle-neck effect has not yet occurred. The method of applying these indentations when the bottle-neck effect occurs will be discussed later on in this paper. The resulting characteristic curves for the two materials are presented in Figures. 2a and 2b.

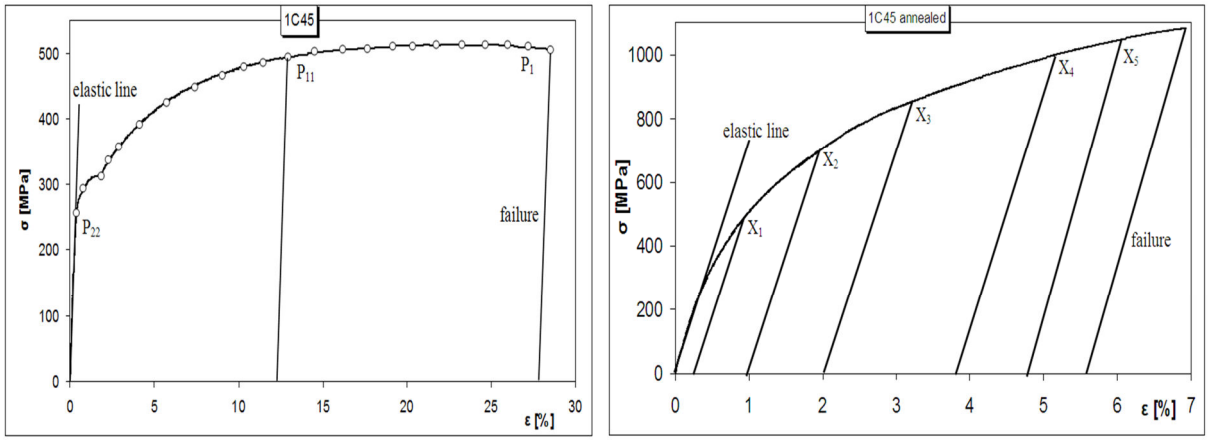

a) 1C45 (1.053) steel b) 1C45 (1.053) annealed steel

Fig. 2 - Typical stress-strain dependence for the studied steel 1C45 (1.053)

In fact, 23 tensile tests were conducted for the 1C45 (1.053) steel specimens: one tests up to failure, whereas the other 22 were stopped at loading levels (P_1 to P_{22}) represented on the curve in Figure 2a. The 1C45 (1.053) steel specimens, tested in various stages of plastic strain, can be seen in Figure 3. Specimen 1 was subjected to tensile up to failure, specimen 2

was subjected to tensile at significant plastic strains, very close to failure, and specimen 22 was subjected to tensile in the elastic domain. For the 1C45 (1.053) annealed steel, 6 tests were conducted, one of which until failure (Figure 2b).

Fig. 3 - The 1C45 (1.053) steel specimens subjected to strain, in various stages of plastic strain

Figure 4 illustrates the stress-strain dependence curve for the 1C45 (1.053) material, with a stop of the load increasing at a certain level of tensile stress (corresponding to point P_{11} from Figure 2a), followed by the load decreasing to zero. It is well known that, when loaded beyond the yield stress level of its material, any tensile specimen has parts of its material volume that are plastically strained, while other regions of its volume are elastically strained. As a consequence, one can consider that the entire strain of the specimen ($\varepsilon_T \rightarrow \Delta l_T$) could be obtained as the sum of the cumulated elastic ($\varepsilon_E \rightarrow \Delta l_E$) and respectively plastic ($\varepsilon_P \rightarrow \Delta l_p$) strains. As it could be observed in Figure 4, the area noted with A_p (which will appear in certain discussions below), could be considered as corresponding to the permanent plastic strain of a certain tensile specimen, which is established after the complete unloading of the respective sample. It can be seen that the A_p area is limited (to the right) by a straight line which is approximately parallel to the initial elastic line of the load-displacement curve.

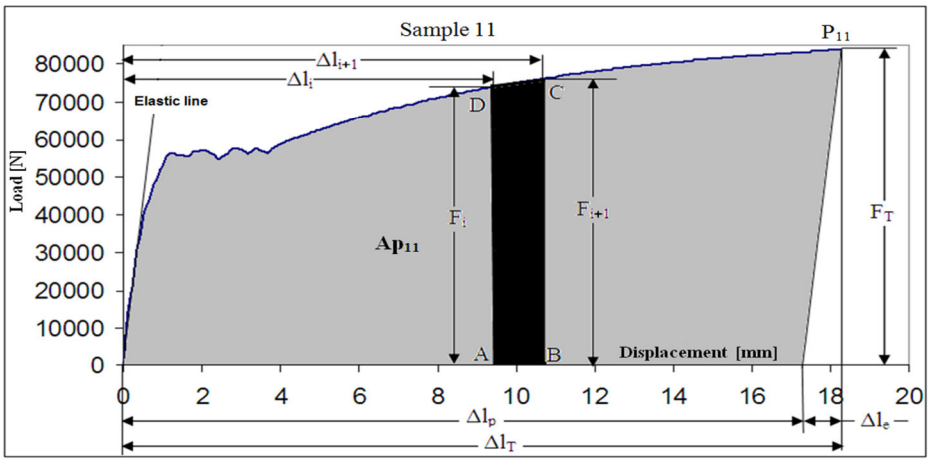

Fig. 4 - Definition of the area (A_p) of the plastic strain domain (1C45 (1.053))

Regarding the calculus of A_p area, one can use the load-displacement data base file that is supplied by the computer of the testing machine. The A_p area can be calculated as the total area upon the load-displacement curve till the P_j point, corresponding to the stress value at which the tensile test was interrupted:

$$Ap_j = \sum_i \left[\left(\frac{(F_{i+1} + F_i) \cdot (\Delta l_{i+1} - \Delta l_i)}{2} \right) \right] - \left(\frac{F_T \cdot \Delta l_E}{2} \right) \quad (4)$$

As it can be seen in Figure 4, the meaning of the symbols from above is as follows: F_i, F_{i+1}, and Δl_i, Δl_{i+1} are, respectively, the force and displacement levels corresponding to the consecutive points, (i) and (i+1), from the load-displacement dependence curve, and also from the data base file; F_p is the force at the point P_j, and Δl_E is the elastic displacement of the considered specimen till the moment of test interruption. It is obvious that the method described above can be used for calculating the A_p, using data files acquired from all the loaded samples, until a certain degree of plastic deformation occurs. On the other hand, for all the samples that were loaded as mentioned above, Vickers micro hardness tests were conducted. 28 indentations were performed on each sample. The configuration for each set of indentations depended on whether the bottle-neck effect occurs or not. For the samples for which the bottle-neck effect does not occur, the indentation configuration is the one shown in Fig. 4: along the length of the sample (14 indentations on each side). For the samples for which the bottle-neck effect occurs, the indentation configuration is as following: 7 indentations on the 12.5 mm width of the specimen, on the right side, in the immediate vicinity of the area with maximum plastic strain, other 7 indentations for the left side of the specimen, and 14 indentations on the other side of the specimen. For these specimens as well, the value registered in tables 1 and 2 was the maximum value. The results (maximum values) regarding the corresponding Vickers micro hardness values and the plastic strain areas (under the characteristic curves) are also presented in tables 2 and 3. These tables also present the variations of the hardness reported to the initial state before loading, ΔHV.

Table 1 - Average micro hardness values for 1C45 (1.053) steel tensile tested specimen

Unloading point	P_{22}	P_{21}	P_{20}	P_{19}	P_{18}	P_{17}	P_{16}	P_{15}
HV [daN/cm^2]	150	151.5	156.4	154.2	159.3	164.0	164.3	168.8
ΔHV [daN/cm^2]	0	1.5	6.4	4.2	9.3	14	14.3	18,8.
A_p [J]	0	0.59	0.65	1.11	1.61	3.25	3.35	8.64

Table 1 (continued)

Unloading point	P_{14}	P_{13}	P_{12}	P_{11}	P_{10}	P_9	P_8
HV [daN/cm^2]	170.3	172.0	178.3	182.0	196.3	203.8	211.0
ΔHV [daN/cm^2]	20.3	22	28.3	32	46.3	53.8	61
A_p [J]	12.03	20.46	31.67	44.61	63.09	76.90	90.08

Table 1 (continued)

Unloading point	P_7	P_6	P_5	P_4	P_3	P_2	P_1	Failure
HV [daN/cm^2]	213.3	226.3	229.3	232.5	238.0	251.4	260.0	290
ΔHV [daN/cm^2]	63.3	76.3	79.3	82.5	88	101.4	110	140
A_p [J]	105.03	105.69	111.45	123.12	126.41	124.04	130.08	135.29

Table 2 -Average micro hardness values for 1C45 (1.053) annealed steel tensile tested specimen

Unloading point	Elastic	X_1	X_2	X_3	X_4	X_5	Failure
HV [daN/cm^2]	190	236	277	315	415	510	546
ΔHV [daN/cm^2]	0	46	87	125	225	320	356
A_p [J]	0	7.28	16.22	47.06	162.66	179.09	186

Using the data from the tables 1 and 2 from above, one drew the curves of the hardness values as depending on the above-defined A_p area, which are presented in Figures. 5a and 5b. It can be observed that the hardness values increase when the material suffers in its volume areas important plastic deformations. It can be concluded that the hardness values increase in the strain-hardened areas and seem to be proportional to the level of accumulated plastic deformation. On the other hand, it can be seen (Figure 6) that, when tested in tensile, the studied material presents significant amounts of plastic deformation before failure.

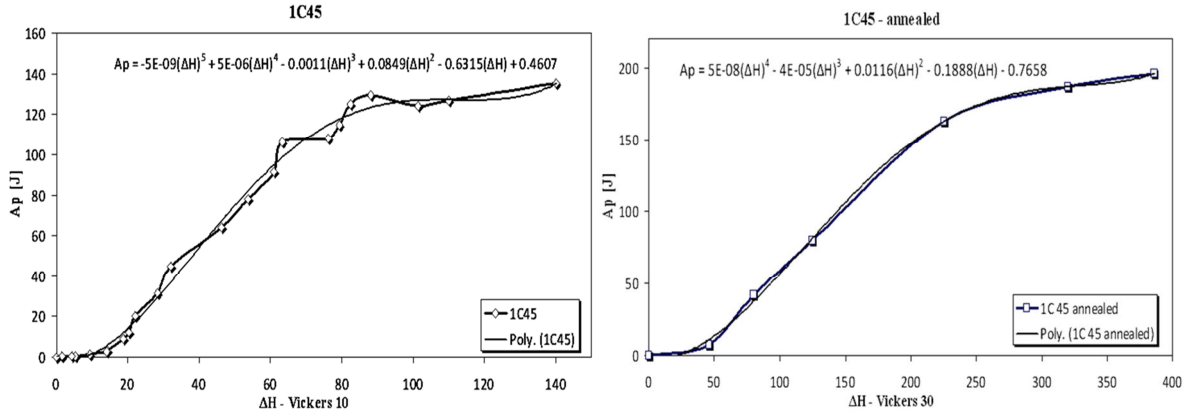

a) 1C45 (1.053) steel b) 1C45 (1.053) annealed steel

Fig. 5 - The variation of (A_p) area of plastic strain domain, in dependence to variations of the hardness (ΔHV)

The hardness values are higher just before failure by 48% (1C45 steel) and respectively by 65% (1C45 annealed steel) when compared to the values that are measured on unloaded material specimens. On the basis of the results mentioned above, one can conclude that the appearance of important plastic deformations in metallic materials leads to significant increases of material hardness values. One may notice that some curves of dependence can be drawn as a correlation of Vickers hardness values with the A_p area, which corresponds to the permanent plastic deformation of a certain material specimen.

For the studied material (and generally for steel), the cited correlation could be mathematically described using a calculus relation of the type:

$$A_p = A\,(\Delta H)^n + B\,(\Delta H)^{n-1} + C\,(\Delta H)^{n-2} + . \qquad (5)$$

where the coefficients A, B, C, etc. could be established from experimental determinations following the model that was described in this paper (see the calculus relations from Figures. 5a and 5b). As a consequence, the resulting curves of dependence (for a certain material) could be used for evaluating, on the basis of Vickers micro hardness tests, the amount of plastic deformation (and the corresponding remaining plastic deformation that could be considered as tolerable before failure) for certain parts or components (which are made of the respective material) which function at its place of working.

TESTING FOR J_{IC} DETERMINATION AND EXPERIMENTAL RESULTS

The program applied for J_{Ic} determination is based on a test of fracture toughness calculation, under quasi-static conditions, in which repeated loading-unloading of the compact tension specimen is performed for forcing the propagation of a crack starting from the pre-cracking previously propagated through fatigue. The test is repeated until the crack attains a pre-specified length of the growth increment or until a pre-specified number of loading-unloading cycles is performed, a moment in which certain results and values of some automatically calculated parameters – among which, the estimated value of integral J, respectively J_Q – are also reported. A sufficiently high number of loading-unloading cycles had been designed, for permitting cracking of the specimen. Consequently, testing were made with the 1C45 (1.053) steel, in normal state, as supplied by its manufacturers, and also on the same steel, yet subjected to thermal annealing. The graphs of force variation versus displacement of the notch's sides, the latter measured with a clip-on-gage extensometer, are plotted in Figures 6a and 6b.

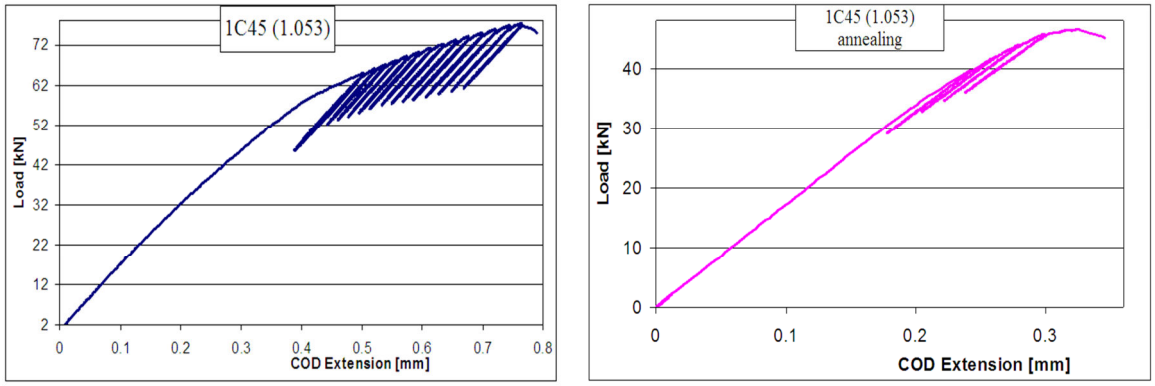

a) 1C45 (1.053) b) 1C45 (1.053) annealed steel

Fig. 6 - Force-extension curves (COD – crack opening displacement)

The observation made was that cracking was produced much earlier in the case of 1C45 (1.053) annealed steel, namely at approximately 48 kN, comparatively with 75 kN for 1C45 (1.053). Also, the number of loadings-unloadings up to cracking is much lower in the case of 1C45 (1.053) annealed steel, which is the result of the embrittlement induced by thermal annealing. Consequently, even if ultimate tensile strength for the annealed steel is higher than that for normal steel (1081 MPa versus 505 MPa), when a fault – in this case, a fissure – appears, the value of the force at which cracking of the annealed steel occurs is lower than for the normal steel, in samples with equal sizes. After loading of the compact specimen through loadings-unloadings up to cracking, the "J_{Ic}-program" loads a series of data on the basis of which the variation graph of integral J versus crack extension may be drawn, Figures. 7a and 7b. Each of the points present on the graphs plotted in Figures. 7a and 7b, represents an equal number of loading-unloading cycles to which the samples had been subjected.

To calculate the estimated value of fracture toughness, J_Q, only the points, occurring between the exclusion straight lines which pass through displacement of 0.15 and 1.5 mm and are parallel to the elasticity straight line, are considered as valid. An approximation curve is plotted through these points. The J_Q value is determined for the point in which the curve of exponential approximation intersects the straight line passing through the extension of the 0.2 mm crack, and is parallel to the elasticity straight line.

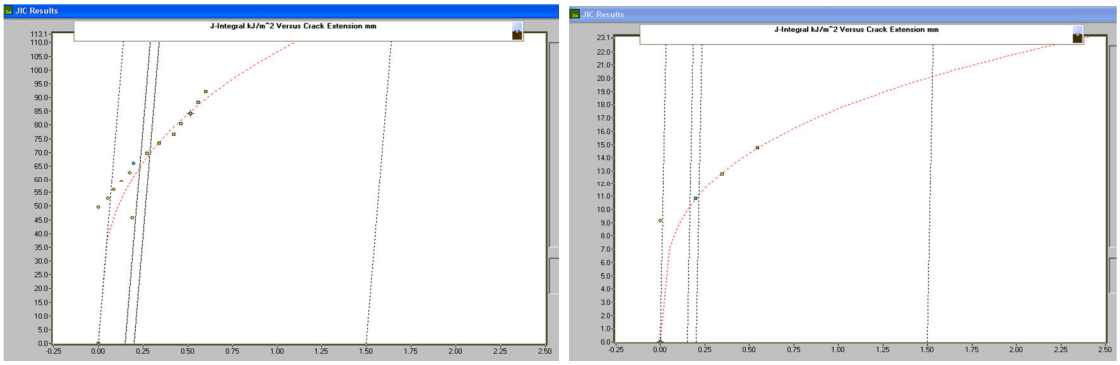

a) 1C45 (1.053) b) 1C45 (1.053) annealed steel

Fig. 7 - Variation of integral J versus crack extension

The validity conditions of the test were met, as also confirmed by the data provided by soft "J_{Ic}", installed on the PC who monitored the testing performed on the INSTRON 8801 machine. In such cases, the estimated values of J_Q may be attributed to fracture toughness J_{Ic}, namely:

$$J_{Ic\text{-}1C45\ (1.053)} = 61.59\ KJ/m^2;\ J_{Ic\text{-}1C45\ (1.053)\text{-}annealing} = 10.97\ KJ/m^2$$

Obviously, fracture toughness is higher in the 1C45 (1.053) normal steel. Actually, the low number of loadings-unloadings up to cracking, for the 1C45 (1.053) annealed steel, supports the idea that the K_{Ic} test would be more appropriate for determining the fracture toughness of this material. However, the present paper applies this type of cracking testing, by means of loading-unloading operations, for observing its effect upon the plastic deformation of the zone in the immediate vicinity of the cracked surfaces.

ASPECT OF THE SURFACES RESULTED THROUGH FRACTURE AT J_{IC} DETERMINATION

As a result of loading-unloading for determining fracture toughness, J_{Ic}, the crack initially introduced through fatigue in the compact tension specimen was propagated up to specimen's cracking. Intense plastic deformations are observed on top of the propagated crack in the 1C45 (1.053) unannealed steel. As shown in Figure 8, the zone with plastic deformations is similar to that presented by Hahn şi Rosenfield (Hahn, 1965).

a) 1C45 (1.053) b) 1C45 (1.053) - annealed

Fig. 8 - Plastic deformations on top of the propagated crack

Crack is initiated at notch level, where the stress intensity factor is high. The effect of stress concentrations is exercised along some distance from the top of the crack. Consequently, the mechanism of crack initiation is similar to that in which propagation initiates at the level of faults. Initiation and propagation of fatigue cracks result from the shift of the sliding bands, known as involving cyclic plastic deformations, as a result of dislocations' movements.

A spatial stress condition is registered on top of the propagated crack. Such an effect of elastic triaxiality determines the form of the zone deformed in the immediate vicinity of the crack. Fatigue occurs at stress amplitudes below the yield strength. At such a low level of stress, plastic deformation is restricted to a reduced number of granules of material. Such micro-plasticity may occur more easily in the granules from the surface of the material, as part of the bonds is absent. Consequently, plastic deformation in the surface granules is more reduced than in the inner ones, so that, on the surface, plastic deformation may appear at lower stresses (Schive, 2001). Cyclic sliding requires a cyclic shear stress.

At microscopic level, tearing stress is not uniformly distributed inside the material. Also, at the level of the crystallographic sliding bands, it differs from one granule to another, according to their size and shape, crystallographic orientation and elastic anisotropy of the material. In some surface granules, these conditions are more favorable for cyclic sliding than in the inner granules. If sliding is produced in a surface granule, a first sliding step will occur on the surface of the material, indicating that another zone of the material is exposed to the environment. Another significant aspect refers to the fact that, during stressing and sliding, some „strengthening" zones appear in the sliding bands. Consequently, on discharging, a higher shear stress, this time in reverse direction, will appear on the same sliding band. Reverse sliding will occur, preferably, within the same sliding band. If cyclic sliding were a wholly reversible process, the fatigue phenomenon described on the basis of sliding, would not have occurred. Creation of a „strengthening" zone in the sliding band is not a reversible process. Consequently, reverse sliding, even if produced in the same sliding band, will occur on parallel adjacent planes. Due to the fewer links present in the area of the free surface, sliding may be easily produced here, which represents a favorable condition for crack' initiation on the surface of the material. As the distribution of stresses is non-homogeneous, its maximum value is registered on the very surface.

The aspect of the surfaces resulted through fracture, as part of the testing for the determination of fracture toughness J_{Ic}, are illustrated in Fig. 9. The differences observed in the aspect of fracture between the two materials are emphasized. The fractured surface of the 1C45 (1.053) steel in normal state is more shiny, showing bigger grains, unlike the 1C45 (1.053)-annealed steel, which presents finer grains on its surface.

Figures 9a and 9b also show the different aspects of the fractured surfaces versus the type of stress and speed of crack propagation. The distinct areas which are presented in these figures are determined both by the behavior of the materials and by the crack growth rate. Consequently, one can observe the area which corresponds to the crack initiation and propagation by fatigue, the area corresponding to the loading-unloading and the area of the sudden crack propagation. A distinct zone should be mentioned as to the aspect of the fractured surfaces and when the crack occurs in the final stage of high-speed propagation. Under such circumstances, it is also assumed that the degree of plastic deformation suffered by the specimen in the immediate vicinity of the fractured surfaces is different.

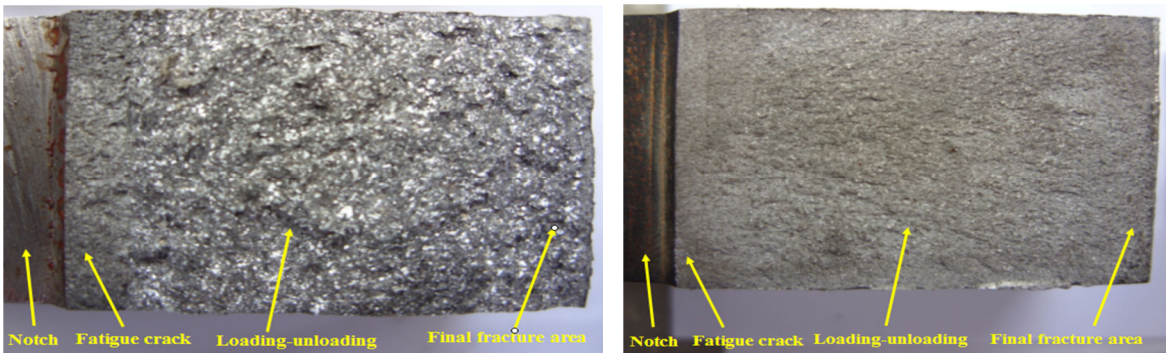

a) 1C45 (1.053) - J_{Ic}; b) annealed 1C45 (1.053) – J_{Ic};

Fig. 9 - Aspect of the fractured surfaces - J_{Ic}

VICKERS MICROHARDNESS TESTINGS PERFORMED IN THE IMMEDIATE VICINITY OF THE FRACTURED SURFACES ON THE BASIS OF THE J_{IC} TESTINGS

Table 3 presents the values which resulted for the Vickers hardness values, determined in the vicinity of the fractured surfaces, and the ΔH hardness variation reported to the prior-deformation state for the 1C45 (1.053) steel. Using the relation presented in Figure 2a and the date in columns 4 and 5 of the table 3, the areas corresponding to the plastic deformation (columns 6 and 7). Consequently, a variation of the Vickers hardness near the fractured surfaces, compared to the initial state, means a higher or lower plastic deformation, reported to the loading in that area.

Table 3 - The Vickers numbers, Vickers variation and A_p variation for 1C45 (1.053) steel

1	2	3	4	5	6	7
Point number	HV row 1	HV row 2	ΔHV row 1	ΔHV row 2	A_p [J] row1	A_p [J] row2
1	265	251	115	101	151.61	137.16
2	264	236	114	86	150.34	124.39
3	242	240	92	90	129.64	127.94
4	266	252	116	102	152.94	138.03
5	266	263	116	113	152.94	149.12
6	257	252	107	102	142.63	138.03
7	254	246	104	96	139.81	132.97
8	257	250	107	100	142.63	136.31
9	258	257	108	107	143.63	142.63
10	262	258	112	108	147.94	143.63

The graphs plotted in Figure 10 show the variations of A_p, the area corresponding to the plastic deformation, along the fractured surfaces, on the two rows, for the 1C45 (1.053) steel.

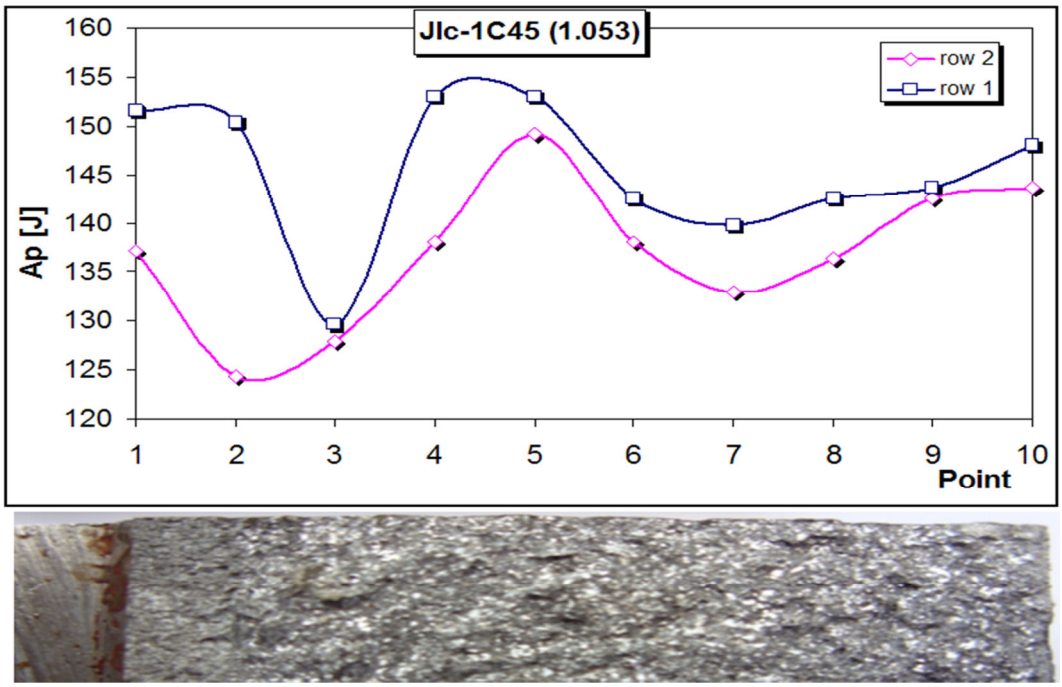

Fig. 10 - Variation of Ap along the fractured surfaces - 1C45 steel - J_{Ic}

The analysis of the graphs plotted in Fig. 10 for the 1C45 (1.053) steel allows the following conclusions:

- The first indentation was performed in the fatigue crack initiation area. Due to the relatively high number of loading cycles used for crack propagation, the plastic deformation degree is higher in this area;

- The second indentation was performed in the fatigue crack propagation area, where the A_p area has lower values than the ones recorded at crack initiation. A mention should be made: the fatigue test was performed with positive stresses only;

- Indentations from 3 to 7 were performed in the loading-unloading area, as presented in Fig. 10a. In this area, increases and decreases of the area corresponding to the plastic deformation are observed. This happens due to tensile-compression loadings applied on the sample. Considering that the indentation points did not exactly follow the loading-unloading areas, it is possible that the variation of the A_p area around points 3-7 is not exactly the same as the real-life value;

- In the final sudden crack propagation area, progressive increases of the A_p area are recorded. It is obvious that the higher value is recorded at the final sample area. In this area, the plastic deformations are high due to the significant increase of stresses;

Table 4 presents the values resulting for the Vickers hardness, determined in the vicinity of the fractured surfaces, for the 1C45 (1.053) annealed steel. The ΔH hardness variation, compared to the state before deformation, and its corresponding A_p values are presented. The correlation between the two was determined using the relation presented in Fig. 2b.

Table 4 - Vickers numbers, Vickers variation and A_p variation for OC45 annealed steel

1	2	3	4	5	6	7
Point number	HV row 1	HV row 2	ΔHV row 1	ΔHV row 2	A_p [J] row1	A_p [J] row2
1	468	426	278	236	101.89	108.11
2	468	428	278	238	101.89	108.37
3	400	378	210	188	100.67	89.55
4	390	329	200	139	96.08	55.58
5	313	304	123	114	43.56	36.92
6	362	313	172	123	79.45	43.56
7	474	411	284	221	98.74	104.68
8	450	426	260	236	107.74	108.11
9	477	404	287	214	96.93	102.27
10	545	529	355	339	5.47	36.57
11	632	563	442	259	101	107.92

By analyzing the graphs plotted in Figure 11 for the 1C45 (1.053)-annealed steel, the following conclusions can be drawn:

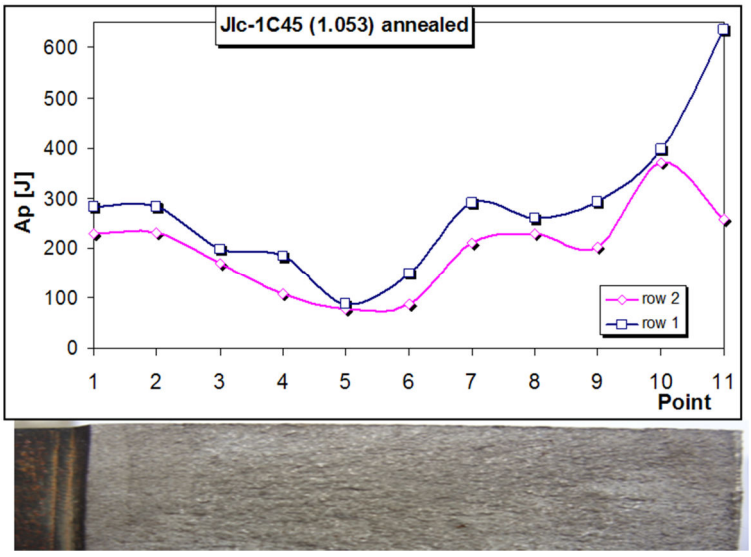

Fig. 11 - Variation of A_p along the fractured surfaces - 1C45 annealed steel- J_{Ic}

- The first two indentations were performed in the fatigue initiation and crack propagation area. We observed that, unlike 1C45 normal steel, there are no differences for the A_p area between the crack initiation and propagation area for the annealed steel. This is due to the fact that, for the annealed steel, a smaller number of cycles was needed for the crack initiation, but also because no major plastic deformation is produced at the top of the crack:

- Indentations 3, 4 and 5 were performed in the loading-unloading area, Figure 8b. A decrease of the A_p area values was observed/
- The following indentation, (until the 9th), were performed in the loading-unloading area. We observe both increases and fluctuations for the A_p area values, reported to the produced loading. Considering that the indentation points did not thoroughly follow the loading-unloading steps, the A_p area variation in this area is not exact. On the other hand, the plastic deformation of the annealed steel is less influenced by loading variations in this area, compared to the normal 1C45 steel.
- In the sudden crack propagation area, the A_p area corresponding to the plastic deformation increases. This increase, for the 1st row, takes place at the end of the sample, where the applied stresses increase, too.

On the other hand, from the data presented in tables 3 and 4, the variation between the maximum and minimum values of the hardness is 24 HC for the normal steel and 232 HV for the annealed steel. This leads to the conclusion that, reported to the initial state, the annealed steel suffers higher plastic deformations.

CONCLUSIONS

As a conclusion, the microhardness is a measure of the degree of plastic deformation suffered by a structural component, when it is loaded beyond the yield limit. This paper takes into consideration loadings derived from using the "J_{Ic}" method in order to produce differentiated plastic deformations. These take place along the surfaces fractured as the result of the Compact Tension Specimen failure. The plastic deformations differ from one area to another along the fractured surfaces, both as a consequence of different loadings and as a following of the crack initiation or propagation method. Considering this observation, for the "J_{Ic}" method, it can be stated that there are five different ways plastic deformation can occur, either by different loading or crack speed propagation.

The five steps in crack development are:

- fatigue crack initiation from notch, at positive stresses
- fatigue crack propagation, at positive stresses
- crack propagation, by static tensile loading
- loading-unloading, at maximum stresses beyond the yield limit
- sudden, final crack propagation

All the steps presented here correlate to different areas of plastic deformation. In addition, the end sample area, where stresses are high, is also taken into consideration.

In this paper, the degree of plastic deformation in each area was determined based on Vickers hardness tests, which took place in the vicinity of the surfaces fractured as a result of the „J_{Ic}" method. As a consequence, for the two materials we had in view, it can be stated that the A_p area corresponding to the plastic deformation is higher at the fatigue crack initiation area. The A_p values decrease in the static loading area and fluctuate in the loading-unloading area. The plastic deformation then increases in the sudden crack propagation area and in the end-sample area.

REFERENCES

[1]-Cahoon JR, Broughton WH, Kutzak AR. The determination of yield strength from hardness measurements, Metallurgical and materials transactions B, 1971, volume 2, number 7, p. 1979-1983.

[2]-Dannenmann E, Wilhelm H, Steck E. Uber den Zusammenhang zwishen Eindring-harte und Umformgrad bei Kaltumformvorgangen. Bander Bleche Rohre, 1968, p. 368-394.

[3]-Hahn GT, Rosenfield AR. Local yielding and extension of a crack under plane stress, Acta Metallurgica 13, 1965, p. 293-306.

[4]-Hernas A. Creep resistance of steel and alloys, Silesian Techn. Univ. Publishers, Gliwice 2001.

[5]-Kim JY, Kang SK, Greer RJ, Kwon D. Evaluating plastic flow properties by characterizing indentation size effect using a sharp indenter, Acta Materialia, 2008, 56, p. 3338–3343.

[6]-Liu Z, Harsono E, Swaddiwudhipong S., Material characterization based on instrumented and simulated indentation tests, International Journal of Applied Mechanics, 2009, Vol. 1, No. 1 p. 61–84

[7]-Pavlina EJ, Van Tyne CJ. Correlation of Yield Strength and Tensile Strength with Hardness for Steels, Journal of Materials Engineering and Performance, 2008, Vol. 17, number 6, p. 888-893.

[8]-Rolfe ST, Barsom JN. Fracture and Fatigue Control in Structures, Ed., Prentice-Hall, New Jersey, 1987.

[9]-Schive J. Fatigue of Structures and Materials. Kluver Academic Publishers, 2001, p. 9-15.
Tabor D., The Hardness and Strength of Metals, Oxford Clarendon Press, 1951.